ELSEVIER

Journal of Nuclear Materials 283–287 (2000) 339–343

journal of nuclear materials

www.elsevier.nl/locate/jnucmat

# Differences in the microstructure of the F82H ferritic/martensitic steel after proton and neutron irradiation

R. Schäublin *, M. Victoria

*Centre of Research in Plasma Physics, Swiss Federal Institute of Technology, Fusion Technology Materials Division, Swiss Confederation, EURATOM Association, Lausanne, 5232 Villigen PSI, Switzerland*

**Abstract**

The microstructure of the F82H steel that is a candidate for the future fusion reactor first wall is investigated. Protons as well as fission neutrons are used to simulate the irradiation effects of the fusion environment. The differences in the He production rates between the two types of irradiation may lead to differences in the irradiation damage of the F82H microstructure. This paper presents a transmission electron microscopy (TEM) study for three different irradiation conditions: (i) in the PIREX facility with 590 MeV protons, (ii) with fission neutrons at the research reactor in Petten and (iii) with 590 MeV protons in PIREX followed by fission neutrons at the reactor in Studsvik. The latter experiment allows us to vary the He production rate for a given irradiation type. Total doses ranged from 0.3 to 10 dpa and temperatures ranged from room temperature to 310°C. 

## 1. Introduction

The low activation ferritic/martensitic steel known as F82H steel [1] is a promising material for the first wall of the future fusion reactor that will suffer irradiation damage from the 14 MeV fusion neutrons. In order to simulate this damage, different types of irradiation are performed using either fission neutrons or accelerated protons. The He production rate for fusion neutron is 13 appm/dpa [2] and about 130 appm/dpa for 590 MeV protons, while it is much lower for fission neutrons. H production rate is higher but is believed to diffuse out of the material. Irradiation is known to drive the microstructure to the formation of He bubbles [3,4], and to a change in the dislocation configuration [4–7]. The effect of He on the mechanical properties is believed to be small [8,9]. Preceding work, however, showed that in F82H at low dose (0.5 dpa) and 250°C, 590 MeV proton irradiation does not significantly change the dislocation configuration [10]. It was also shown that Cr segregates to grain boundaries by the heat treatment, while it is depleted from them by the irradiation [11]. At that stage it was not possible to identify defect clusters with transmission electron microscopy (TEM) for the 0.5 dpa irradiation. In this work, it is proposed to compare the microstructure and mechanical properties of a range of F82H samples that were irradiated in three different conditions: (i) in the PIREX facility with 590 MeV protons at the Paul Scherrer Institute, (ii) with fission neutrons at the research reactor in Petten and (iii) with 590 MeV protons in PIREX followed by fission neutrons in the reactor in Studsvik. The last type of experiment is intended to study the effect of neutron irradiation with the additional amount of He that is produced in larger amounts with protons than with neutrons.

## 2. Experimental

The ferritic/martensitic steel de F82H [1] has a composition of about 7.65 wt% Cr, 2 wt% W, and Mo, Mn, V, Ta, Ti, Si and C below 1 wt% in sum total, and Fe for the balance. The samples were submitted to the heat treatment (0.5 h at 1313 K for normalization and 2 h at 1013 K for tempering) that allows it to be fully martensitic. Table 1 summarizes the various doses, temperatures and irradiation types studied in this work.

* Corresponding author. Tel.: +41-56 310 4082; fax: +41-56 310 4529.

*E-mail address:* robin.schaeublin@psi.ch (R. Schäublin).

0022-3115/00/$ - see front matter 
PII: S0022-3115(00)00223-3

Table 1
F82H irradiation conditions and defect TEM measurement results

| | Irradiation | Dose (dpa) | Temperature (°C) | Defect mean size (nm) | Defect density ($m^{-3}$) | # Defects counted |
|---|---|---|---|---|---|---|
| 1 | Proton | 0.5 | 250 | 1.5 | $2.0\times10^{21}$ | 110 |
| 2 | Proton | 1.0 | 250 | 1.9 | $9.5\times10^{21}$ | 80 |
| 3 | Proton | 1.7 | 40 | 2.4 | $5.0\times10^{21}$ | 121 |
| 4 | Proton + neutron | 0.3 + 0.3 | 250 | 1.9 | $3.0\times10^{21}$ | 90 |
| 5 | Proton + neutron | 0.7 + 0.7 | 250 | 2.0 | $8.0\times10^{21}$ | 170 |
| 6 | Neutron | 0.7 | 250 | 2.2 | $3.0\times10^{21}$ | 150 |
| 7 | Neutron | 2.5 | 250 | 4.3 | $7.0\times10^{22}$ | 584 |
| 8 | Neutron | 10.0 | 310 | 6.9 | $2.8\times10^{22}$ | 320 |

Sample preparation is optimized in order to reduce magnetism and radioactivity by using the following procedure. Samples are punched to produce 1 mm disks, which are then inserted in a 1 mm hole punched into the center of a 3 mm 316 stainless steel disk. The assembly is then glued with epoxy and mechanically polished to about 100 μm before the usual electropolishing. Relatively to a sample that was punched to 3 mm, no modification of the structure that could have been induced by the 1 mm punching could be detected. Time between sample preparation and its transfer in the TEM is about 10 min and samples are kept in water-free ethanol. Samples older than 4 h are generally discarded. These are important steps that minimize oxidation.

TEM was performed at 200 kV on a JEOL2010 using the weak beam technique [12]. The conditions selected are $g(4g)$ and $g(6g)$ with $g$ $\{0\,1\,1\}$ (deviation parameter $s = 0.08$ and 0.13 $nm^{-1}$, respectively). It appears that the quality of the surface of the thin foil is of crucial importance for the observation of defect clusters that are about 1 nm in size. The TEM observations reveal a detrimental background contrast from surface features that presents a uniform grainy texture which characteristic size is a little less than 1 nm. A series of weak beam conditions with $g = \{0\,1\,1\}$ was tested in order to define the most appropriate ones. The reason why the $g(4g)$ and $g(6g)$ conditions were selected, when possible, is that when higher conditions are used resolution is improved but contrast is smeared by surface feature contrasts. The comparison of the images taken with two different conditions allows recording most of the defect clusters present in the foil.

## 3. Results

Irradiation of F82H with either protons or neutrons leads, for the doses considered in this work, to hardening. Previous investigations [13] showed that irradiation induced damage is clearly visible in TEM for doses higher than about 1 dpa. It shows as black dots that are related to point defect clusters. It appears that in the case of lower doses the damage is difficult to see in the TEM [10]. In this work, improved sample preparation technique and handling as described above allow observing defects for the irradiation with protons to 0.5 dpa at 250°C. Results of the defect size and density for the different irradiation conditions are presented in Table 1.

Fig. 1 illustrates the various types of defect configurations that are induced by the irradiations in the F82H. The left column of Fig. 1 shows $(0\,1\,1)$ $g(4g)$ weak beam images of the F82H irradiated with neutrons. The respective irradiation conditions correspond to the doses of 0.7, 2.5 and 10 dpa for Figs. 1(a), (c) and (e). F82H irradiated with neutrons to 0.7 dpa at 250°C present in Fig. 1(a) dot contrasts, which are visible only nearby the edge of the sample that is visible on the right of the image (black vertical line). In thicker areas of the sample the image is sufficiently blurred by the inelastic electrons to cancel out the contrast of small crystal defects. At a dose of 2.5 dpa the F82H material presents large enough clusters to be visible in any region of the thin sample. Interestingly, it appears that the cluster size and density distributions are spatially heterogeneous. Fig. 1(b) shows, in the upper left part of the boundary running across the image, the case of a martensite lath observed in bright field using a $(0\,1\,1)$-type diffraction vector. The cluster size and density are larger close to the martensite lath boundary, which is decorated by carbides, than in plain regions that are free of dislocations and carbides, as in the bottom right corner of the image. Close to the lath boundary the clusters are clearly resolved as loops when using a weak beam condition, while they remain as unidentified clusters far from it (Fig. 1(c)). At a dose of 10 dpa, F82H presents a more homogeneous cluster distribution. Dislocation loops are clearly resolved, as displayed in Fig. 1(e).

Irradiation with protons to a dose of 1.7 dpa at room temperature leads to visible defects in the TEM, as shown in the $(0\,1\,1)$ $g(4g)$ weak beam image of Fig. 1(d). The visual comparison with the neutron irradiation at a dose of the same order, 2.5 dpa, indicates that defects are smaller. This might be due to the lower dose and to the lower irradiation temperature as well. In the case of the cumulative dose experiment, whereby a dose of

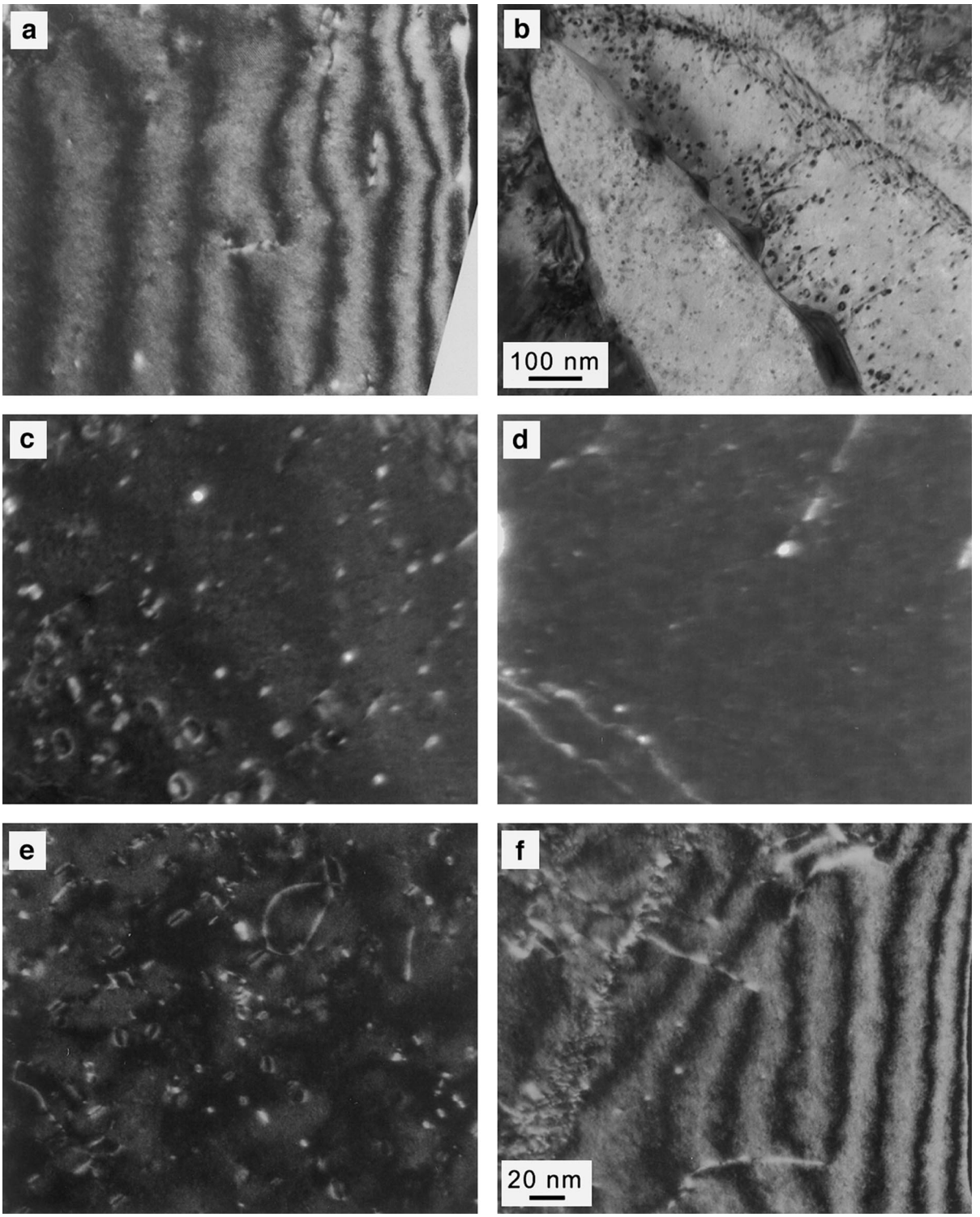


Fig. 1. TEM micrographs of F82H ferritic/martensitic steel illustrating the irradiation conditions with protons and/or neutrons. Left column corresponds to neutron irradiation conditions using weak beam $g(4g)$ condition, $g = \{0\,1\,1\}$, foil normal $\langle \mathrm{FN} \rangle \approx \langle 1\ 1\ 1 \rangle$. Respective conditions correspond to the dose of (a) 0.7 dpa (irradiation # 6 in Table 1), (c) 2.5 dpa (# 7) and (e) 10 dpa (# 8). (b) TEM Bright field, $g = \{0\,1\,1\}$, $\mathrm{FN} \approx \langle 1\ 1\ 1 \rangle$, micrograph of F82H with 2.5 dpa (# 7), (d) weak beam $g(4g)$ image, $g = \{0\,1\,1\}$, of F82H irradiated at 1.7 dpa at 40°C (# 3) and (f) weak beam $g(4g)$ image, $g = \{0\,1\,1\}$, $\mathrm{FN} \approx \langle 1\ 1\ 1 \rangle$, of F82H irradiated at 0.7 dpa with protons and 0.7 dpa with neutrons at 250°C (# 5).

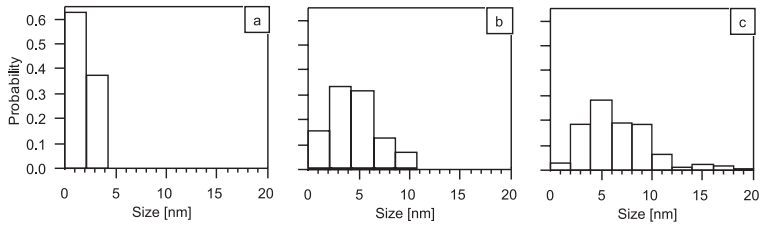


Fig. 2. Size distributions of the defect clusters in neutron irradiated F82H at (a) 0.7 dpa (irradiation # 6), (b) 2.5 dpa (# 7) and (c) 10 dpa (# 8).

0.7 dpa with protons and a dose of 0.7 dpa with neutrons were applied at 250°C to the F82H, it appears that the damage exhibits a similar visibility, Fig. 1(f), to that of the case of the single irradiation with neutrons to a dose of 0.7 dpa at 250°C in the same TEM conditions.

The size distributions for the pure neutron irradiations (#6, 7 and 8), Fig. 2, indicate an increase in the mean size of the irradiation induced defect clusters. In addition, there is with increasing dose a decrease in the relative number of the smaller clusters to the advantage of larger ones as clearly seen when comparing the size distribution in the 0.7 dpa irradiation, Fig. 2(a), to that for 10 dpa irradiation (Fig. 2(c)). The increase in dose from 2.5 to 10 dpa broadens the size distribution, respectively, Figs. 2(b) and (c), to larger sizes. The defect densities in Table 1 present an increase when going from 0.7 to 2.5 dpa. As previously shown, no difference in defect accumulation has been found between 590 MeV protons and neutrons at $T_{irr} = 0.2$–$0.3\ T_M$ (melting point) [14]. There is a decrease when increasing further to 10 dpa. This indicates in correlation with the former fact that the larger clusters will grow at the expense of new smaller ones, which means also that the defect density has reached saturation at a dose value between 2.5 and 10 dpa.

The fact that the defect clusters in F82H are difficult to see as compared to the case of Cu for instance where defects are clearly visible from doses of less than $10^{-4}$ dpa [15] indicates that displacement cascades induce smaller intracascade clusters. In addition, a recent molecular dynamics simulation study [16] showed that sessile clusters are not stable. They would therefore transform to a glissile configuration that allows them to escape to sinks such as dislocations, martensite lath boundaries, grain boundaries and carbides. With increasing dose, new clusters can contribute to the growth of already present defect clusters. This is confirmed by the present observations whereby at the larger dose fewer smaller clusters are created.

Carbides are amorphized in the case of the irradiation with protons to a dose of 1.7 dpa at room temperature. In all other cases it appears that the carbides remain crystalline. This indicates, as in the case of another ferritic/martensitic steel denominated OPTIMAX A [17], that it is the temperature that controls the amorphization under irradiation. When the irradiation temperature is higher than 250°C carbides are not amorphized by the irradiation. Defocusing experiments in the TEM [18] performed in all samples did not reveal cavities. This indicates a good resistance of the F82H to irradiation induced swelling, for doses up to the highest investigated dose of 10 dpa.

## 4. Conclusions

1. In the ferritic/martensitic steel F82H irradiated with protons, the defect density does not seem to have reached saturation for the studied doses ($\leqslant 1.7$ dpa). In the case of the neutron irradiations, defect density has reached saturation at a dose value between 2.5 and 10 dpa. Coarsening of dislocation loops is operative above 2.5 dpa.
2. Carbides are amorphized in the case of the irradiation with protons to a dose of 1.7 dpa at room temperature. In all other cases it appears that the carbides remain crystalline. Temperature is the controlling parameter for amorphization.
3. There were no observable cavities, even at the highest studied dose of 10 dpa. This indicates a good resistance of the F82H to swelling.

## Acknowledgements

The authors wish to thank David Gelles for fruitful advices in TEM and sample preparation. Emil van Osch, of NRG, Petten, The Netherlands, and Anders Lind, of Studsvik, Sweden, are acknowledged for their fruitful collaboration. Paul Scherrer Institut is acknowledged for the overall use of the facilities.

## References

[1] M. Tamura, H. Hayakawa, M. Tanimura, A. Hishinuma, T. Kondo, J. Nucl. Mater. 141–143 (1986) 1067.

[2] M.S. Wechsler, D.R. Davidson, L.R. Greenwood, W.F. Sommer, in: F.A. Garner, J.S. Perrin (Eds.), Effects of Radiation on Materials: Proceedings of the 12th Conference, ASTM STP 870, ASTM 1985, p. 1189.
[3] E.A. Little, D.A. Stow, J. Nucl. Mater. 87 (1979) 25.
[4] D.S. Gelles, J. Nucl. Mater. 108&109 (1982) 515.
[5] Y. Katoh, A. Kohyama, D.S. Gelles, J. Nucl. Mater. 225 (1995) 154.
[6] R. Bullough, M.H. Wood, E.A. Little, in: D. Kramer, H.R. Brager, J.S. Perrin (Eds.), Effects of Radiation on Materials: Proceedings of the 10th Conference, ASTM STP 725, ASTM 1981, p. 593.
[7] E.A. Little, R. Bullough, M.H. Wood, Proc. Roy. Soc. London A 372 (1980) 565.
[8] K.K. Bae, K. Ehrlich, A. Möslang, J. Nucl. Mater. 191–194 (1992) 905.
[9] K. Shiba, M. Suzuki, A. Hishinuma, J.E. Pawel, in: D.S. Gelles, R.K. Nanstad, A.S. Kumar, E.A. Little (Eds.), Effects of Radiation on Materials: Proceedings of the 10th Conference, ASTM STP 1270, ASTM 1996, p. 753.
[10] R. Schäublin, P. Spätig, M. Victoria, J. Nucl. Mater. 258–263 (1998) 1178.
[11] R. Schäublin, P. Spätig, M. Victoria, J. Nucl. Mater. 258–263 (1998) 1350.
[12] D.J.H. Cockayne, I.L.F. Ray, M.J. Whelan, Philos. Mag. A 20 (1969) 1265.
[13] R. Schäublin, M. Victoria, Mater. Res. Soc. Symp. 540 (1999) 597.
[14] M. Victoria, N. Baluc, C. Bailat, Y. Dai, M.I. Luppo, R. Schäublin, B.N. Singh, J. Nucl. Mater. 276 (1–3) (2000) 114.
[15] Y. Dai, M. Victoria, Acta. Metall. 45 (1997) 3495.
[16] Y.N. Osetsky, D.J. Bacon, A. Serra, B.N. Singh, S.I. Golubov, J. Nucl. Mater. 276 (2000) 65.
[17] N. Baluc, R. Schäublin, C. Bailat, F. Paschoud, M. Victoria, these Proceedings, p. 731.
[18] M. Rühle, M. Wilkens, Cryst. Latt. Def. 6 (1975) 129.